

Characterizing Impact Factors on the Performance of Data Assimilation for Hydroclimatic Predictions through Multilevel Factorial Analysis

X. D. Lyu¹ and Y. R. Fan¹ *

¹Department of Civil and Environmental Engineering, Brunel University, London, Uxbridge, Middlesex UB8 3PH, United Kingdom

Received 14 April 2020; revised 25 May 2020; accepted 29 June 2020; published online 06 February 2021

ABSTRACT. In this study, the multi-level factorial analysis approach is employed to characterize the major impact factors on the performances of different data assimilation schemes. Four data assimilation methods, including EnKF and PF methods, and two integrated data assimilation methods are adopted for real-time hydrological prediction through a conceptual rainfall-runoff model in a catchment of Jing River. Different uncertainty scenarios for model inputs and outputs, as well as streamflow observations are tested through the multilevel factorial analysis to track the dominant impacts factors on the performances of data assimilation approaches. The multi-level factorial results suggest that, for different data assimilation schemes, the impacts from stochastic perturbations in model inputs, outputs and streamflow observations are different and some of them may be statistically insignificant. But the impact for one factor is generally dependent upon the others and scenarios with extreme stochastic perturbations (low or high) may more likely result in a good performance for all data assimilation schemes.

Keywords: data assimilation, ensemble kalman filter, particle filter, multi-level factorial analysis, uncertainty

1. Introduction

In a hydrologic prediction context, model simulations or predictions are subject to various uncertainties stemming from model inputs (i.e., forcing data), model structures, and model parameters (Liu et al., 2012). Sequential data assimilation (SDA) techniques are widely used for explicitly dealing with various uncertainties and for optimally merging observations into uncertain model predictions (Reichle et al., 2002; Moradkhani et al., 2005a; Vrugt et al., 2005; Clark et al., 2008; Xie and Zhang, 2013). In SDA, the state variables, and parameters in a hydrologic model can be continuously updated when new measurements are available through sequential data assimilation techniques, and such a process can highly improve the model predictions. The ensemble Kalman filter (EnKF) and particle filter (PF) methods are two of the most widely used sequential data assimilation schemes. The approaches of EnKF, PF and their variants have been widely used in hydrologic data assimilation (e.g., Moradkhani et al., 2005a, b; Parrish et al., 2012; Pathiraja et al., 2016a, b; Fan et al., 2015a, b; 2016; 2017a, b).

For a data assimilation scheme (e.g., EnKF or PF), it has been demonstrated that its “optimality” depends critically on the reliability of error estimates for the inputs and the model itself, as well as the proper consideration of interdependencies and interactions among the uncertain model components and/or

observations (Crow and Van Loon, 2006; Moradkhani et al., 2006 a, b; Hong et al., 2006; Liu et al., 2012). Consequently, accounting for uncertainties in model inputs and predictions is crucial for providing reliable hydrological predictions. Some approaches have been developed to deal with uncertainties in model inputs, streamflow observations and model outputs, such as the stochastic perturbation method (Steiner, 1996; Crow and Van Loon, 2006; Pauwels and De Lannoy, 2006; Weerts and El Serafy, 2006; Clark et al., 2008; Li, et., 2008; Komma et al., 2008; Pan and Wood, 2009; Tan et al., 2011), conditional simulation methods (Clark and Slater, 2006; G zinger and B  rdossy, 2009), inverse methods (Vrugt et al., 2003), and multi-model ensembles (e.g., Georgakakos et al., 2004). Among them the stochastic perturbation method is widely used, in which, uncertainties in model inputs, streamflow observations and model predictions are reflected through the addition of stochastic perturbations based on order-of-magnitude considerations (Liu et al., 2012). Some research works have addressed the impacts of stochastic perturbations on the performance of data assimilation schemes. For instance, Moradkhani et al. (2005a) introduced hyper-parameters to denote the proportionality between the variances in the Gaussian distribution noise and the magnitude of the variables and further analyzed the performance of EnKF under different combinations of the hyper-parameters. These stochastic perturbations may influence the performance of prediction accuracy in data assimilation process. However, few research works have been reported to characterize the main effects of stochastic perturbations and their interactions on the performances for different data assimilation schemes.

Consequently, this research aims to characterize the im-

* Corresponding author. Tel.: +44 (0)1895 265717.
E-mail address: yurui.fan@brunel.ac.uk (Y. R. Fan).

pacts of random errors on the performance of different data assimilation schemes through a multi-level factorial analysis approach. In detail, four data assimilation schemes are tested through a real case study in Jing River basin, including traditional EnKF and PF, as well as two new integrated data assimilation schemes (i.e., the coupled EnKF and PF (CEnPF) and parallelized EnKF and PF (PEnPF)) proposed in our previous work (Fan et al., 2017a). Different stochastic perturbation scenarios in forcing data, model predictions and observations are assumed. The multi-level factorial analysis is adopted to characterize the main and interactive effects of stochastic perturbations on the performances of different data assimilation schemes.

2. Methods

2.1. Data Assimilation Approaches

There are a number of data assimilation approaches for uncertainty quantification and reduction in hydrologic prediction, in which ensemble Kalman filter (EnKF) and the particle filter (PF) are two of the most widely used sequential data assimilation schemes. The EnKF and its variants use the Monte Carlo method to approximate the error statistics, and then compute an approximate Kalman gain matrix for updating model and state variables. In comparison, the particle filter (PF) method also uses random samples (i.e., particles) to approximate the distributions of the model state, but instead of changing the particle values, the particle weights are updated forward by using sequential Monte Carlo (SMC) simulation.

Based on EnKF and PF, some integrated data assimilation approaches have been proposed, such as the coupled EnKF and PF (CEnPF) method and the parallelized EnKF and PF (PEnPF) method proposed in Fan et al. (2017a). The CEnPF sequentially updates model parameters and states through Kalman update equations, and then corrects the updated states and parameters again through PF procedure to eliminate abnormal or insignificant state and parameters and replace them by significant ones based on a sampling importance resampling procedure. The PEnPF approach simultaneously updates model states and parameters in parallel through EnKF and PF in each time step, and chooses the better estimates as the posterior distributions. Detailed procedures for EnKF, PF, CEnPF and PEnPF can be referred to relevant studies (Moradkhani et al., 2005a, b; Fan et al., 2017a; Li et al., 2010).

2.2. Uncertainties in Sequential Data Assimilation Processes

In data assimilation, stochastic perturbations are usually added into model inputs, streamflow observations and model predictions to account for their inherent uncertainties. Such perturbations are generally assumed to be proportional to the order-of-magnitude considerations. In such a process, the uncertainty is represented by adding perturbation or random error drawn from a predefined distribution with a mean value of zero and a variance being the order-of-magnitude considerations. For instance, the Gaussian random perturbations in forcing data and model predictions can be expressed as (Moradkhani et al.,

2005a):

$$u_i = u_i + \xi_i, \xi_i \sim N(0, \Sigma_i^u) \quad \text{and} \quad \Sigma_i^u = \gamma u_i \quad (1)$$

$$y_i = y_i + \eta_i, \eta_i \sim N(0, \Sigma_i^y) \quad \text{and} \quad \Sigma_i^y = \rho y_i \quad (2)$$

where γ and ρ are the proportionality factor considered as hyper-parameters. Some research works have been reported to consider the impacts of these proportionality factors (e.g., Moradkhani et al., 2005b, Leisenring and Moradkhani, 2012). However, the interactions between these proportionality factors are not well explored. To address the above issue, a multi-level factorial analysis is proposed to explore the single and interactive effects of the proportionality factors in model prediction noise, forcing data noise and observation noise on the performances of different data assimilation schemes.

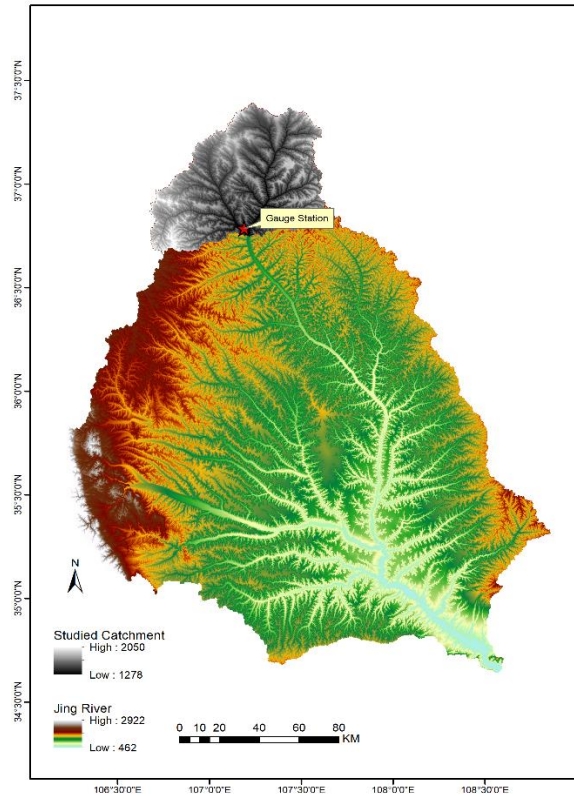


Figure 1. The location of the studied catchment.

2.3. Multi-level Factorial Analysis for Characterizing Interactions among Uncertainty Components

Factorial analysis is widely used for visualizing the single effects of factors with discrete values (or levels) and their interactive effects on a response variable, in which a factorial design is employed to account for all combinations of the levels of factors (Fan et al., 2020a, b, 2021). For example, consider a system model is subject to three factors A, B, and C, in which factor A has a level, factor B has b levels, and factor C has c levels. A complete experiment considering all levels of the three factors

with n replicates will have $abcn$ observations, and the effect model for such a factorial experiment can be expressed as:

$$y_{ijkl} = \mu + \eta_i + \xi_j + \gamma_k + (\eta\xi)_{ij} + (\eta\gamma)_{ik} + (\xi\gamma)_{jk} + (\eta\xi\gamma)_{ijk} + \varepsilon_{ijkl} \quad (3)$$

$$\begin{cases} i = 1, 2, \dots, a \\ j = 1, 2, \dots, b \\ k = 1, 2, \dots, c \\ l = 1, 2, \dots, n \end{cases}$$

where μ denotes the overall mean effect; η_i , ξ_j , γ_k respectively denote the effect of factor A at the i th level, factor B at the j th level, and factor C at the k th level; $(\eta\xi)_{ij}$, $(\eta\gamma)_{ik}$ and $(\xi\gamma)_{jk}$ indicate the interactions of factors A and B, factors A and C, and factors B and C, respectively; $(\eta\xi\gamma)_{ijk}$ denotes the interaction among factors A, B, and C; ε_{ijkl} means the random error component. According to Montgomery (2000), the treatment effects are defined from the overall mean, so we have $\sum_{i=1}^a \eta_i = 0$, $\sum_{j=1}^b \xi_j = 0$, $\sum_{k=1}^c \gamma_k = 0$, $\sum_{i=1}^a (\eta\xi)_{ij} = \sum_{j=1}^b (\eta\xi)_{ij} = 0$, $\sum_{i=1}^a (\eta\gamma)_{ik} = \sum_{k=1}^c (\eta\gamma)_{ik} = 0$, $\sum_{j=1}^b (\xi\gamma)_{jk} = \sum_{k=1}^c (\xi\gamma)_{jk} = 0$, and $\sum_{i=1}^a (\eta\xi\gamma)_{ijk} = \sum_{j=1}^b (\eta\xi\gamma)_{ijk} = \sum_{k=1}^c (\eta\xi\gamma)_{ijk} = 0$. The statistical significance of each factor and the interactions between different factors can be characterized by the F statistic obtained as follows:

$$F_{n_r} = \frac{MS_{n_r}}{MS_e} = \frac{SS_{n_r} / (v_{n_r} - 1)}{SS_e / [r(n - 1)]} \quad (4)$$

$$F_{n_1, n_2, \dots, n_q} = \frac{MS_{n_1, n_2, \dots, n_q}}{MS_e} = \frac{SS_{n_1, n_2, \dots, n_q} / [(v_{n_1} - 1)(v_{n_2} - 1) \dots (v_{n_q} - 1)]}{SS_e / [r(n - 1)]} \quad (5)$$

where n_r means the factor of interest ($r = 1, 2, \dots, q$), v_{n_r} indicates the number of levels of factor n_r , r denotes the product of numbers of levels for all factors, and n means the number of replicates. MS_{n_r} , $MS_{n_1, n_2, \dots, n_q}$ and MS_e denote the mean squares of individual factors, interaction among factors and the error component, respectively. The sum of squares for single factors (SS_{n_r}), interactions between two factors (SS_{n_u, n_w}), interactions among three factors (SS_{n_u, n_w, n_z}), and the error component (SS_e) can be calculated:

$$SS_{n_r} = \frac{1}{rn / v_{n_r}} \sum_{i=1}^{v_{n_r}} y_i^2 - \frac{y^2}{rn} \quad (6)$$

$$SS_{n_u, n_w} = \frac{1}{rn / (v_{n_u} v_{n_w})} \sum_{i=1}^{v_{n_u}} \sum_{j=1}^{v_{n_w}} y_{ij}^2 - \frac{y^2}{rn} - SS_{n_u} - SS_{n_w} \quad (7)$$

$$SS_{n_u, n_w, n_z} = \frac{1}{n} \sum_{i=1}^{v_{n_u}} \sum_{j=1}^{v_{n_w}} \sum_{k=1}^{v_{n_z}} y_{ijk}^2 - \frac{y^2}{rn} - SS_{n_u} - SS_{n_w} - SS_{n_z} - SS_{n_u, n_w} - SS_{n_u, n_z} - SS_{n_w, n_z} \quad (8)$$

$$SS_T = \sum_{i=1}^{v_{n_u}} \sum_{j=1}^{v_{n_w}} \sum_{k=1}^{v_{n_z}} \sum_{l=1}^n y_{ijkl}^2 - \frac{y^2}{rn} \quad (9)$$

$$SS_e = SS_T - SS_{n_u} - SS_{n_w} - SS_{n_z} - SS_{n_u, n_w} - SS_{n_u, n_z} - SS_{n_w, n_z} - SS_{n_u, n_w, n_z} \quad (10)$$

where y_i , y_{ij} , and y_{ijk} denote the total of all observations under the i th level of one factor, the ij th interaction between two factors, and the ijk th interaction among three factors, respectively; SS_T denotes the total sum of squares; y means the grand total of all observations. These statistics are collected in ANOVA that signifies a decomposition of the variance into contributing components and characterizes the differences between two or more means by analyzing variances from multiple sources (Wang et al., 2015; Fan et al., 2015a; Fu et al., 2021; Dong et al., 2021).

In this study, a multi-level factorial design will be employed to visualize the effects of stochastic perturbations in different data assimilation schemes with multiple levels. In this factorial design, at every combination of stochastic perturbation level, an experimental run will be conducted, and this will lead to a total run of the product of the number of levels in each factor. To be more specific, a 3^k factorial design is proposed for screening the effects of the proportionality factors in model prediction, observation and forcing data on the performances of different data assimilation approaches. The 3^k factorial design outperforms regular two-level designs in studying the effects of several independent variables (factors) with multiple levels on a dependent variable (response), especially when a curvilinear relationship exists between the design factors and the response (Wang et al., 2015).

3. Case Study

3.1. Model and Site Description

Once The case study of the catchment, located in the north part of the Jing River watershed presented in Figure 1, is employed to reveal the impacts of random errors in forcing data, output measurements and model prediction on the performance of data assimilation schemes. The detailed description of the Jing River watershed and the used catchment is provided in Fan et al. (2017a). For the hydrologic model used in this study, the Hymod proposed by Moore (2007) is employed, which is a non-linear rainfall-runoff conceptual model which can be run in a minute/hour/daily time step. Five parameters are involved in this model and two inputs (i.e., precipitation and potential evapotranspiration) are required to force this model.

3.2. Stochastic Perturbation Scenarios

To account for uncertainties in the forcing data, output measurements and model prediction, the random perturbation approach is used based on order-of-magnitude considerations. Three error scenarios for model inputs, streamflow observations and model predictions are considered to reveal the main and interactive impacts of stochastic perturbations on the perfor-

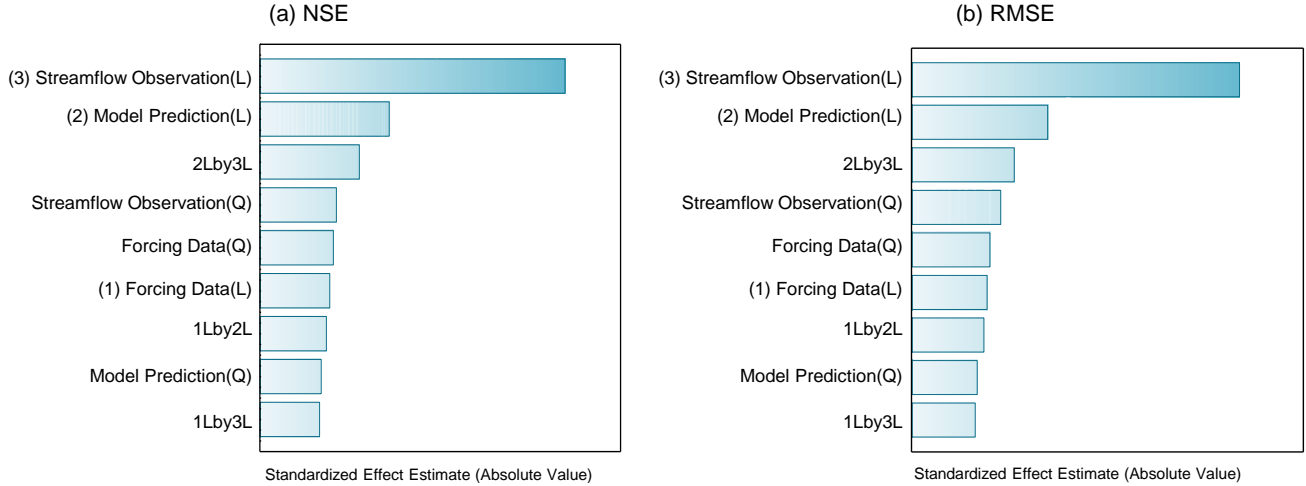


Figure 2. Pareto chart of standardized effects in terms of NSE (a) and RMSE (b) for EnKF. (1)Forcing Data(L) means the linear main effect from random error in forcing data; (2)Model Prediction(L) means the linear main effect of random error in model prediction; (3)Streamflow Observation(L) means the linear main effect from random error in streamflow prediction; Forcing Data(Q), Model Prediction(Q), Streamflow Observation(Q) denote the quadratic main effects for random errors in the three factors, respectively; 1Lby2L means the interaction of factors (1) and (2); 1Lby3L means the interaction of factors (1) and (3); 2Lby3L means the interaction of factors (2) and (3).

mances on hydrological predictions for different data assimilation schemes. In detail, proportionality factors are assumed to be 0.1, 0.2 and 0.3 to account for uncertainties in the forcing data, streamflow observations and model predictions. Moreover, Gaussian noise is adopted to reflect uncertainties in the potential evapotranspiration, and streamflow observations, which can be expressed by Equation (1). Also, uncertainty in model predictions is reflected by Gaussian noise as expressed by Equation (2). Owing to the multiplicative nature of precipitation and only zero or positive values are possible, the precipitation data were log-normally varied with a heteroscedastic assumption (i.e., the variance estimate was scaled by the magnitude) as follows (Leisenring and Moradkhani, 2012):

$$\mu_{\ln P} = \ln[P_t^2 / \sqrt{P_t^2 + (\gamma_p P_t)^2}] \quad (11)$$

$$\sigma_{\ln P} = \sqrt{\ln[(\gamma_p P_t)^2 / P_t^2 + 1]} \quad (12)$$

$$\tilde{P}_t^i = \exp(\mu_{\ln P} + w_p^i \sigma_{\ln P}^2 / 2) \quad w_p^i \sim N(0,1) \quad (13)$$

where \tilde{P}_t^i is the precipitation for sample i at time t , P_t is the measured precipitation at time t , γ_p is a variance scaling factor for precipitation data, which was assumed to be 0.1, 0.2 and 0.3.

4. Results Analysis

A 3^k factorial analysis is proposed to explore the single and interactive effects of uncertain components in the forcing data, model predictions and streamflow observations on the performances of EnKF, PF, CEnPF and PEnPF. In detail, the proportionality factor values (i.e., 0.1, 0.2 and 0.3) are assumed to in-

dicade the low, medium, and high levels of the uncertain components in forcing data, model predictions and streamflow observations, leading to a 3^3 factorial design. The factorial design had a single replicate without the consideration of “noise”, in which, three and higher-way interactions were neglected, and their mean squares were thus combined to provide an internal estimate of error in the ANOVA (Wang et al., 2015). This is based on the sparsity-of-effects principle stating that a system is usually dominated by main effects and two-way interactions, and interactions involving three or more factors are rare and can thus be neglected (Montgomery, 2000). Consequently, there are total of 27 runs in this factorial design experiment, as shown in Table 1. This experiment is capable of making a clear test of main effects and two-way interactions of stochastic perturbations on different data assimilation schemes. A three-year time period (1979 ~ 1981) observations are adopted in the north part of Jing River basin to characterize the impacts of stochastic perturbations in inputs, observations and model predictions on the performance of different data assimilation schemes.

4.1. Impacts of Stochastic Perturbations on EnKF

Table 2 shows the performances of the EnKF approach under different combinations of stochastic perturbations in forcing data, model predictions and streamflow observations. In general, the EnKF provides satisfactory predictions under different random error scenarios, with the NSE value ranging within [0.53, 0.70] and the RMSE value ranging within [9.80, 12.27]. Table 3 shows the results of the ANOVA for the EnKF approach. In the ANOVA table, the terms with P-values being less than 0.05 are statistically significant, and vice versa when the P value is greater than 0.05. The results indicate that the random errors in streamflow observations and model predictions have significant main effects on the performance of EnKF, while

the random perturbations in forcing data are statistically insignificant in this case. Furthermore, the two-way interaction effect can be interpreted as half the difference between the linear effect of one factor at the low and high levels of the other factors. The results in Table 3 reveal that the interaction between the random errors in model predictions and streamflow observation poses a significant impact on the performance of EnKF, while the other two interactions have minimal influence on EnKF, which may be due to the insignificant main effect of the random error in the forcing data. Three Pareto charts of standardized effects are presented in Figure 2. The Pareto chart is a powerful tool for visualizing the individual and joint effects of all factors on model outputs. The rank is displayed by bars in a descending order. Thus, factor (3) (i.e., random error in streamflow observations) is identified as the most significant factor for EnKF, followed by factor (2) which is the random error in model prediction. The symbol (L) represents linear effects. Moreover, the interaction between factors (2) and (3) is ranked as the third most significant factor. Factor (1) (i.e., random error in forcing data) is not as significant as the above two factors. These results are resonant with the conclusions drawn from the ANOVA table.

Table 1. The 3³ Fractional Factorial Design Matrix with Detailed Stochastic Perturbations

Runs	Forcing Data	Model Predictions	Streamflow Observations
1	0.2	0.1	0.2
2	0.2	0.1	0.1
3	0.2	0.3	0.3
4	0.1	0.2	0.2
5	0.3	0.3	0.2
6	0.3	0.1	0.1
7	0.2	0.3	0.1
8	0.3	0.3	0.3
9	0.2	0.3	0.2
10	0.3	0.2	0.2
11	0.3	0.1	0.2
12	0.2	0.2	0.2
13	0.1	0.2	0.1
14	0.1	0.1	0.2
15	0.3	0.2	0.3
16	0.1	0.1	0.1
17	0.1	0.3	0.3
18	0.2	0.2	0.3
19	0.3	0.1	0.3
20	0.2	0.1	0.3
21	0.3	0.3	0.1
22	0.1	0.2	0.3
23	0.1	0.3	0.2
24	0.2	0.2	0.1
25	0.1	0.1	0.3
26	0.3	0.2	0.1
27	0.1	0.3	0.1

To visualize the influence of the factors on the response and to compare the relative magnitude of the effects, Figures (3a) and (3b) present the main effects plot of the three factors

at three chosen levels. This plot shows that the performance of EnKF changes remarkably, depending on the levels of the random errors in streamflow observations with the steepest line. This reveals that random errors in streamflow observations have the largest main effect on EnKF, with a decrease of NSE value from 0.68 to 0.62 and then to 0.56 across low, medium, and high levels of the random errors in streamflow observations. In comparison, random errors in the forcing data has a smaller contribution to the performance of EnKF because its line is almost horizontal (parallel to the x-axis) in the main effects plot. Figures (3c) and (3d) present the full interactions plot matrix with three factors at three random error levels for the performance of EnKF, in which each pair of factors provides two panels. Considering the right subplot in the second row of Figure (3c) as an example, this reveals that the change in the performance of EnKF differs across the three levels of the random error in model prediction, depending on the level of random error in streamflow observations, implying that an interaction between these two factors occurs and their effects are dependent upon each other. The best NSE value of 0.68 would be generated when the random error in streamflow observations is at its lowest level and the random error in model predictions is at its medium level. The other subplots also indicate interactions among streamflow observations vs. forcing data and model predictions vs. forcing data, but these interactions do not seem to be as strong as the interaction between streamflow observation vs. model prediction.

Figure 4 shows the fitted response surfaces with contour plots of the interactions among the three factors. These plots show second-order (quadratic) effects on the performance of EnKF and provide a general idea on the performance of EnKF at various random error settings in forcing data, model predictions and streamflow observations. The 3D surfaces of streamflow observations and model predictions show the most significant changes in NSE and RMSE values. Moreover, these two 3D surfaces reveal a significant increasing trend of NSE towards the right side and a decreasing trend of RMSE in the same direction. This indicates that the performance of EnKF can be improved while reducing the random error in streamflow observations, but at the same time the change of random error in model predictions does not have a significant influence.

For this case study application, the random error in streamflow observations poses the most significant impact on the performance of the EnKF, followed by the random error in model predictions, and the impact of random error in the forcing data is statistically insignificant. Interactions occur among the three factors but the interaction between random errors in streamflow observations and model predictions is most significant. Moreover, the performance of the EnKF can be improved when the random error in streamflow observations is decreased. But the impact from model predictions is not significant when the random error in streamflow observations is at the lowest level.

4.2. Impacts of Stochastic Perturbations on PF

The NSE and RMSE values of PF under different combinations of stochastic perturbations in forcing data, model pre-

dictions and streamflow observations are also presented in Table 2. Compared with EnKF, the performance of PF usually differs if the same random error scenario is employed. This may be due to the difference in parameter and state evolution mechanism in EnKF and PF. In general, PF performs better than EnKF

in several random error scenarios with the best NSE value reaching approximately 0.8. Table 4 shows the results of the ANOVA for PF. It can be concluded that random errors in the forcing data, model predictions and streamflow observations are statistically insignificant, since all the P-value are larger

Table 2. Performance of Different Data Assimilation Schemes in the Factorial Design Experiment

Runs	EnKF		PF		CEnPF		PEnPF	
	NSE	RMSE	NSE	RMSE	NSE	RMSE	NSE	RMSE
1	0.595	11.364	0.626	11.141	0.635	10.799	0.753	8.871
2	0.677	10.150	0.590	11.412	0.624	10.959	0.814	7.703
3	0.567	11.752	0.393	13.918	0.682	10.079	0.672	10.222
4	0.607	11.192	0.666	10.251	0.654	10.512	0.767	8.624
5	0.650	10.574	0.617	11.022	0.669	10.282	0.855	6.803
6	0.687	9.998	0.636	10.653	0.645	10.642	0.829	7.392
7	0.709	9.697	0.617	10.975	0.726	9.354	0.811	7.771
8	0.618	11.036	0.703	9.729	0.651	10.555	0.837	7.206
9	0.624	10.954	0.617	11.033	0.689	9.962	0.810	7.792
10	0.616	11.075	0.616	11.001	0.662	10.388	0.822	7.546
11	0.590	11.433	0.671	10.206	0.613	11.108	0.876	6.299
12	0.609	11.164	0.621	10.990	0.630	10.872	0.801	7.962
13	0.699	9.797	0.576	11.619	0.650	10.575	0.622	10.977
14	0.591	11.429	0.561	11.826	0.633	10.823	0.786	8.265
15	0.579	11.595	0.648	10.401	0.614	11.092	0.859	6.719
16	0.681	10.090	0.685	9.958	0.707	9.673	0.742	9.068
17	0.585	11.512	0.584	11.448	0.839	7.160	0.733	9.228
18	0.555	11.920	0.518	12.398	0.613	11.118	0.537	12.153
19	0.534	12.193	0.587	11.419	0.615	11.090	0.841	7.120
20	0.519	12.387	0.797	8.057	0.638	10.753	0.453	13.215
21	0.712	9.614	0.722	8.996	0.656	10.480	0.669	10.279
22	0.572	11.687	0.509	12.511	0.648	10.599	0.741	9.083
23	0.641	10.702	0.579	11.551	0.692	9.912	0.631	10.854
24	0.685	10.025	0.681	9.983	0.663	10.374	0.694	9.876
25	0.528	12.268	0.652	10.506	0.614	11.096	0.846	7.004
26	0.689	9.961	0.588	11.854	0.644	10.664	0.848	6.974
27	0.670	10.262	0.672	10.119	0.712	9.580	0.714	9.550

Table 3. Results of ANOVA for EnKF

	Degree of Freedom	SS	MS	F	P
NSE					
forcing data	2	0.0008717	0.000436	4.19	0.057
model prediction	2	0.0066508	0.003325	32	0
streamflow observation	2	0.0706461	0.035323	339.92	0
forcing data*model prediction	4	0.0004217	0.000105	1.01	0.455
forcing data*streamflow observation	4	0.0006558	0.000164	1.58	0.27
model prediction* streamflow observation	4	0.0028379	0.00071	6.83	0.011
Error	8	0.0008313	0.000104		
Total	26	0.0829153			
RMSE					
forcing data	2	0.17357	0.08678	3.56	0.078
model prediction	2	1.30266	0.65133	26.73	0
streamflow observation	2	15.08235	7.54118	309.5	0
forcing data*model prediction	4	0.09335	0.02334	0.96	0.48
forcing data*streamflow observation	4	0.12087	0.03022	1.24	0.367
model prediction* streamflow observation	4	0.51814	0.12953	5.32	0.022
Error	8	0.19493	0.02437		
Total	26	17.48586			

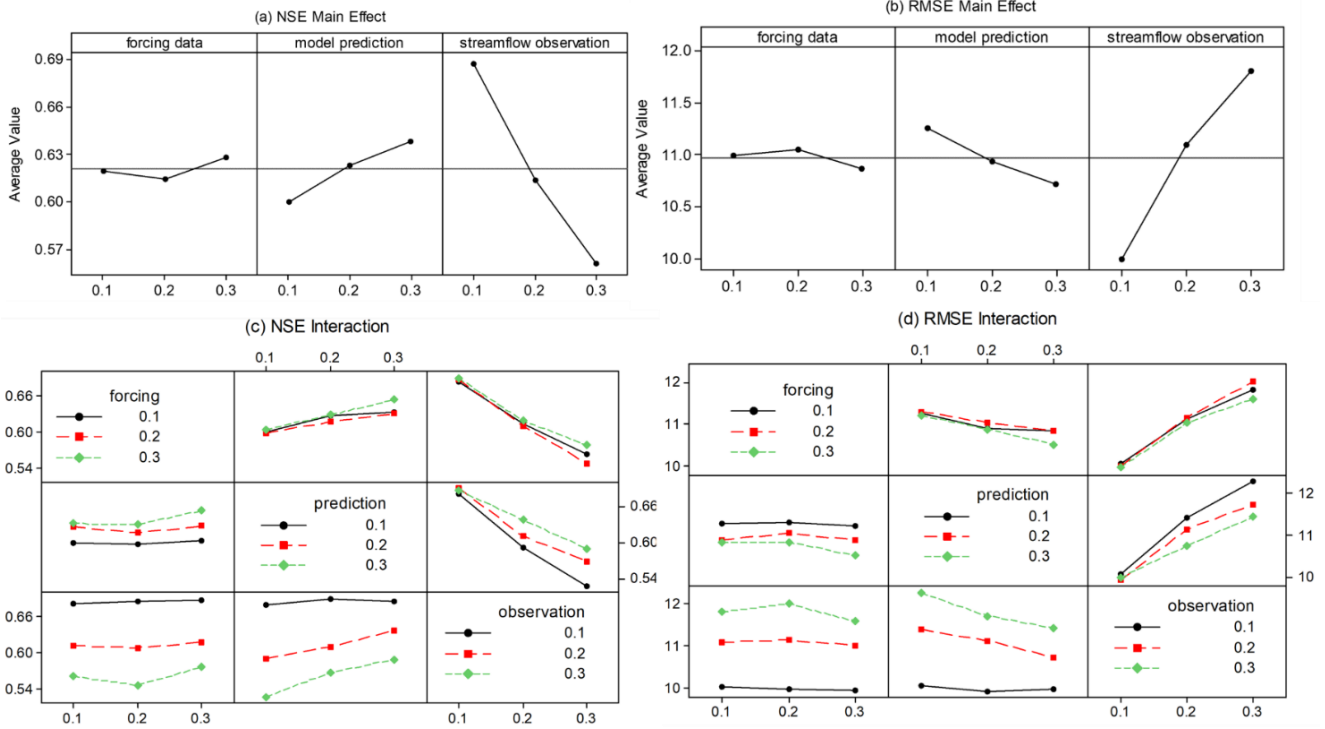


Figure 3. Main and interactive effects for the stochastic perturbations on the performance of EnKF approach. Figures (9a) and (9b) indicate that the proportionality factor in streamflow observation poses the most significant impact on EnKF with a lower proportionality factor value leading to a better performance. The intersection of the three lines in Figures (9c) and (9d) indicate that interactive effects occur for two factors at three levels. The broken lines imply the nonlinear relationship between stochastic perturbations and model performance.

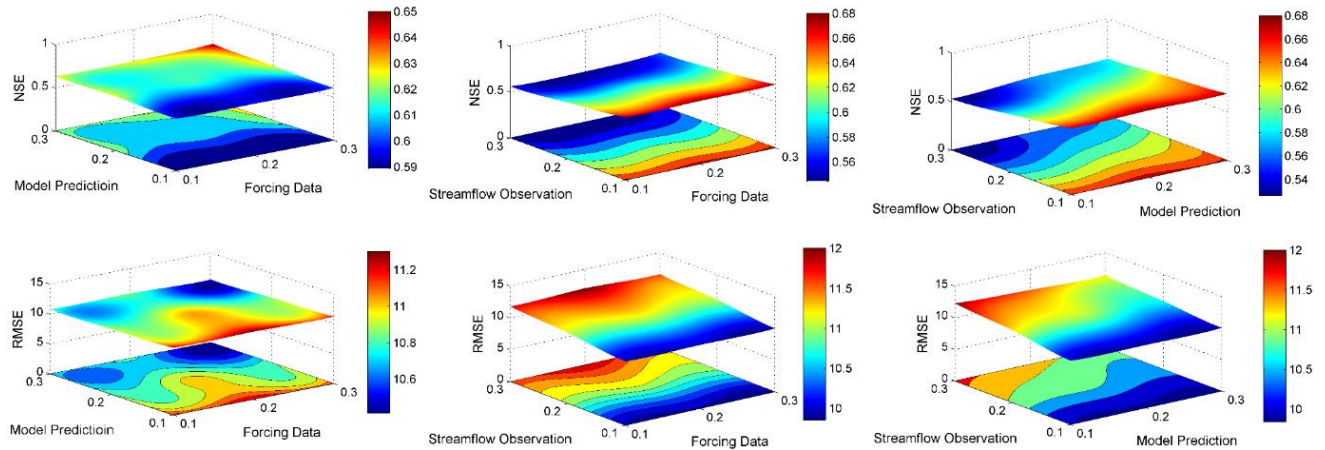


Figure 4. Fitted response surfaces with contour plots for the interactions among the three stochastic perturbation factors for EnKF.

than 0.5. Moreover, the interactions among the three factors (i.e., forcing data, model predictions and streamflow observations) do not have significant impacts on the performance of PF, since their main effects are insignificant. Even though the random errors do not have noticeable impacts on the performance of PF in this case, their individual and joint effects can also be ranked by the Pareto chart, as shown in Figure 5. The impact rank for PF is generally different with the rank for EnKF, except that factor (3) (i.e., random error in streamflow observa-

tions) is also identified as the most significant factor for PF. Particularly, all the effects for PF are statistically insignificant, while the first three effects for EnKF are statistically significant, as shown in Table 3.

Figure 6 shows the visualization of the main effects of the three factors at three chosen levels and their interactions plot matrix. This reveals that the random error in streamflow observation has the largest main effect on PF, which is the same for the performance of EnKF. Moreover, the random errors in forc-

Table 4. Results of ANOVA for PF

NSE	Degree of Freedom	SS	MS	F	P
forcing data	2	0.00753	0.003765	0.43	0.667
model prediction	2	0.009	0.0045	0.51	0.619
streamflow observation	2	0.007897	0.003949	0.45	0.655
forcing data*model prediction	4	0.02607	0.006517	0.74	0.592
forcing data*streamflow observation	4	0.004996	0.001249	0.14	0.962
model prediction* streamflow observation	4	0.025469	0.006367	0.72	0.602
Error	8	0.070759	0.008845		
Total	26	0.151721			

RMSE	Degree of Freedom	SS	MS	F	P
forcing data	2	0.943	0.471	0.23	0.802
model prediction	2	2.103	1.052	0.51	0.62
streamflow observation	2	0.831	0.416	0.2	0.822
forcing data*model prediction	4	4.417	1.104	0.53	0.716
forcing data*streamflow observation	4	1.352	0.338	0.16	0.951
model prediction* streamflow observation	4	5.234	1.308	0.63	0.654
Error	8	16.596	2.074		
Total	26	31.475			

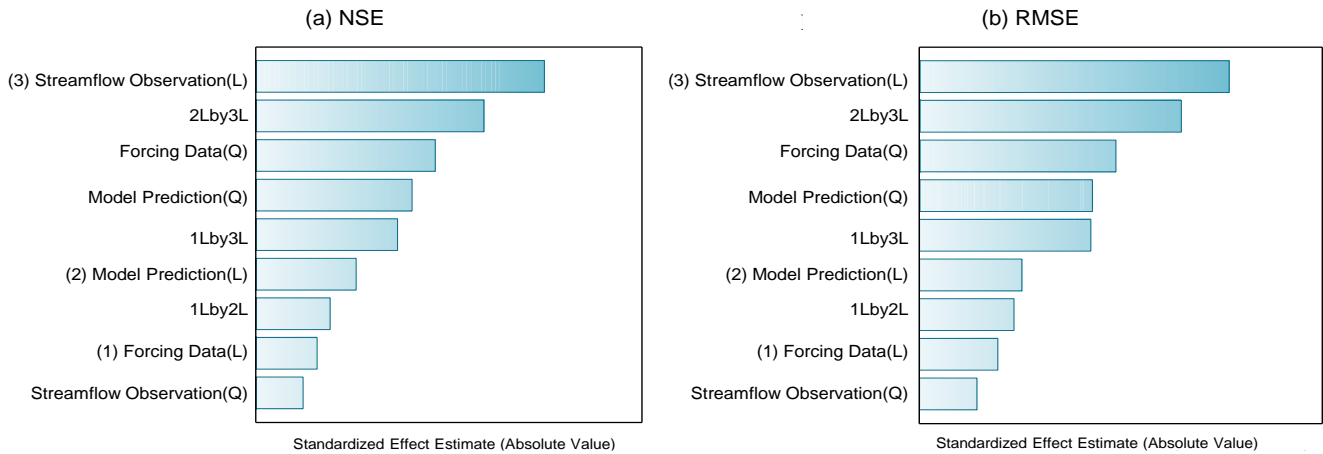


Figure 5. Pareto chart of standardized effects in terms of NSE (a) and RMSE (b) for PF. The random error in streamflow observation influences the performance of PF most significantly, followed by the interaction of factors (2) and (3). In general, the rank based on NSE is the same as the rank through RMSE for PF. However, all the above effects are statistically insignificant.

ing data and model predictions have smaller contributions to the performance of PF than the random error in streamflow observations. However, these two random errors seem to pose relatively more impacts on PF than those on the performance of EnKF as shown in Figures (3a) and (3b). Furthermore, Figure 6 also indicates that the full interactions from the three factors on PF show a different pattern from those on EnKF, but interactions between these three factors occur and their effects are dependent upon each other. Figure 7 shows the fitted response surfaces with contour plots of the interactions of the three factors on the performance of PF. These plots show quadratic effects produced by the three selected factors. The 3D surfaces indicate that PF usually reaches better results in the corner or edge areas. Moreover, different combinations of random errors may lead to a similar performance of PF. These results suggest that extreme random error scenarios may be employed to improve the performance of PF in this case, and these scenarios

have multiple options.

In general, the impacts of the random errors on the performance of PF are different from those factors on the performance of EnKF. These impacts are statistically insignificant for the performance of PF in this case. Also, the detailed rank of these factors and their interaction plot matrix are generally different from those for EnKF. The fitted response surfaces for the interactions for PF show different changing trends with the variation of random errors. All these differences may result from the different evolution mechanisms between PF and EnKF.

4.3. Impacts of Stochastic Perturbations on CEnPF

Table 2 presents the performances of CEnPF under different combinations of stochastic perturbations in forcing data, model predictions and streamflow observations. The results indicate that the performance of CEnPF is dependent upon these

stochastic perturbations. In general, the performance of CEnPF performs better than the traditional EnKF and PF approaches with the NSE value fluctuating within [0.614, 0.839], and the corresponding RMSE value varying within [7.16, 11.096]. Table 5 shows the results of ANOVA for CEnPF. This table shows different conclusions from the ANOVA results for EnKF and PF. It can be concluded that random error in model predictions

has a statistically significant impact on the performance of CEnPF, since the corresponding P-value is less than 0.05. The other two factors and all the interactions among the three factors show statistically insignificant impacts. Figure 8 exhibits the individual and joint effects of the three factors ranked by the Pareto chart. The linear main effect of random error in model predictions has the most significant impact on the performance

Table 5. Results of ANOVA for CEnPF

NSE	Degree of Freedom	SS	MS	F	P
forcing data	2	0.008333	0.004166	2.68	0.129
model prediction	2	0.023919	0.011959	7.69	0.014
streamflow observation	2	0.001345	0.000673	0.43	0.663
forcing data*model prediction	4	0.005253	0.001313	0.84	0.535
forcing data*streamflow observation	4	0.003417	0.000854	0.55	0.706
model prediction* streamflow observation	4	0.004826	0.001207	0.78	0.571
Error	8	0.012449	0.001556		
Total	26	0.059542			

RMSE	Degree of Freedom	SS	MS	F	P
forcing data	2	2.3538	1.1769	2.51	0.143
model prediction	2	6.3073	3.1536	6.72	0.019
streamflow observation	2	0.3086	0.1543	0.33	0.729
forcing data*model prediction	4	1.6699	0.4175	0.89	0.512
forcing data*streamflow observation	4	1.146	0.2865	0.61	0.667
model prediction* streamflow observation	4	1.4932	0.3733	0.8	0.56
Error	8	3.7532	0.4691		
Total	26	17.032			

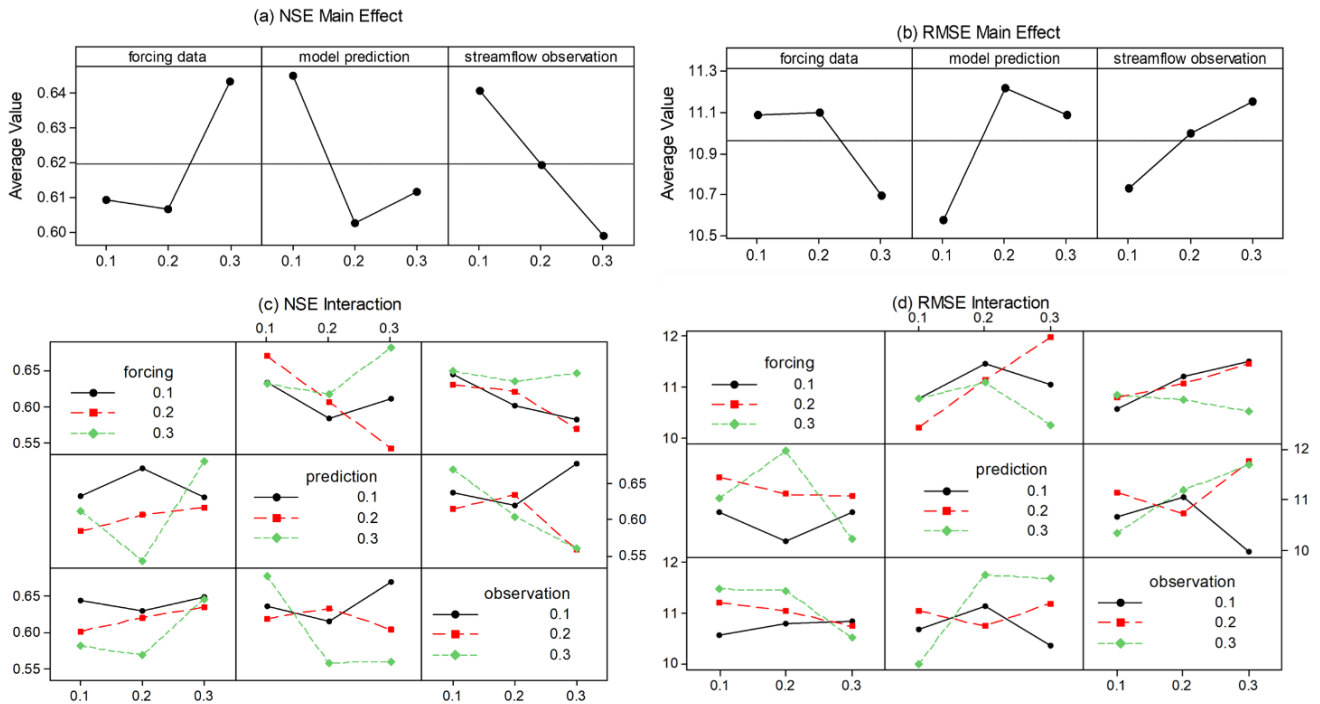


Figure 6. Main and interactive effects for the stochastic perturbations on the performance of the PF approach. Figures (12a) and (12b) indicate that the proportionality factor in streamflow observation poses the most significant impact on PF with a lower proportionality factor value leading to a better performance. The intersection of the three lines in Figures (12c) and (12d) indicate that interactive effects occur for two factors at three levels. The broken lines imply the nonlinear relationship between stochastic perturbations and model performance.

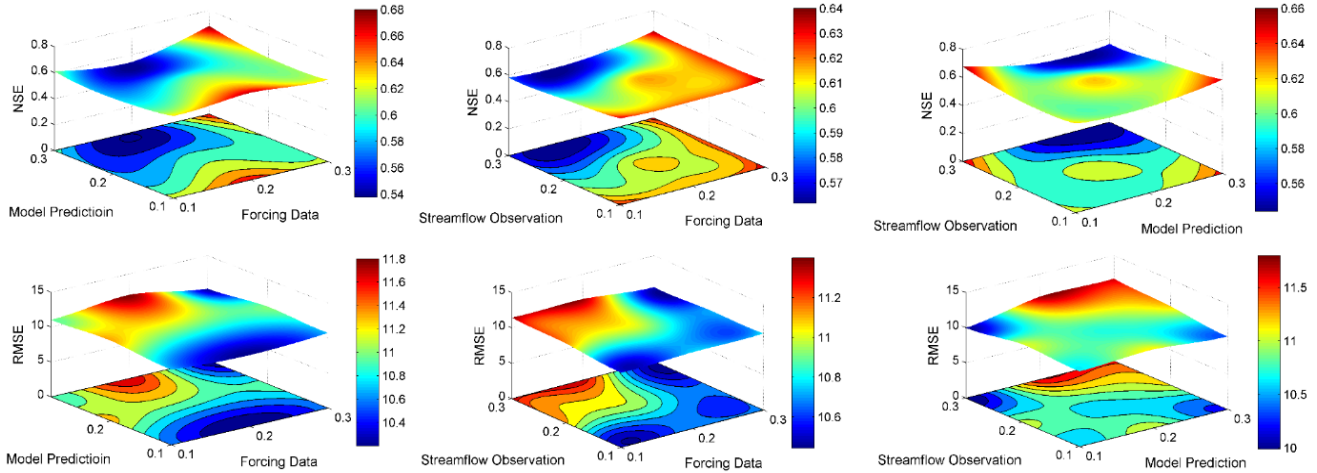


Figure 7. Fitted response surfaces with contour plots for the interactions among the three stochastic perturbation factors for PF.

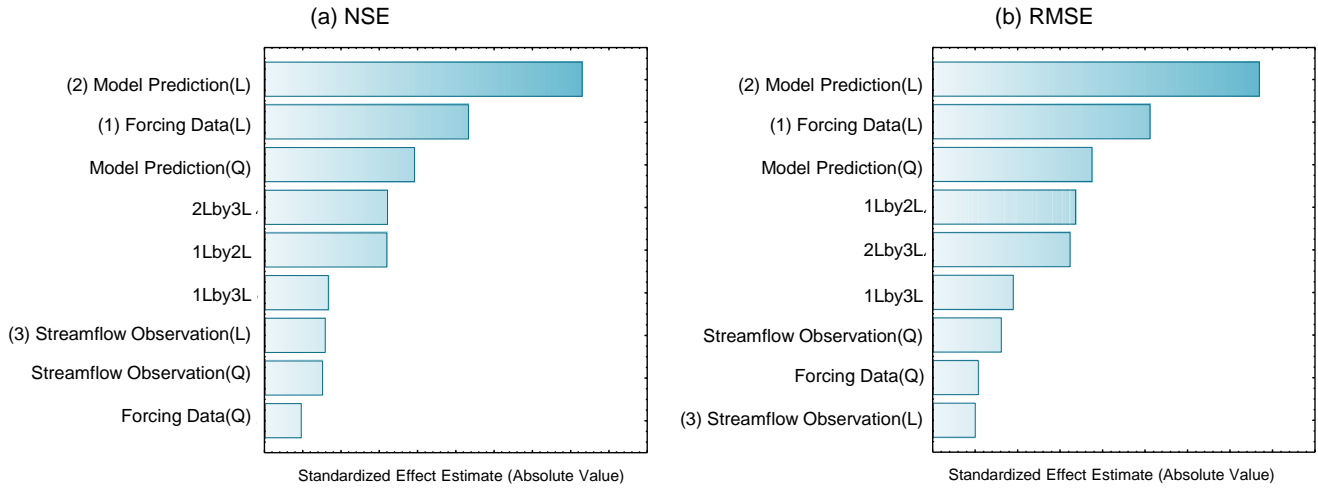


Figure 8. Pareto chart of standardized effects in terms of NSE (a) and RMSE (b) for CEnPF. The random error in model prediction (i.e., factor (2)) influences the performance of CEnPF most significantly, followed by random error in forcing data (i.e., factor (1)). The rank based on NSE is almost the same as the rank based on RMSE except some differences for minor impacts. However, only the first one (i.e., the randomness in model prediction) is statistically significant.

of CEnPF, followed by the linear main effect from forcing data, and the quadratic effect of model predictions. The Pareto charts for NSE and RMSE are similar except for slight differences in the rank of some insignificant effects.

Figure 9 presents the main effects plot for the three proportionality factors at three levels, and their interaction plot matrix. This can be helpful for visualizing the magnitudes of the main effects of factors and their interactions. In the main effects plots (i.e., Figures (9a) and (9b)), it can be concluded that the proportionality factor in the random error for model predictions has the greatest magnitude of the main effect upon the performance of CEnPF, and a higher proportionality factor will result in a better performance of CEnPF. Moreover, the random error in streamflow observations has the smallest contribution to the performance of CEnPF because its line is almost horizontal (parallel to the x-axis) in the main effects plot. These results are different from the main effect plots for EnKF and PF, in which

the random error in streamflow observations has a largest contribution. Figures (9c) and (9d) present the full interactions plot matrix for the three proportionality factors at three levels, which show different characteristics from the interaction plots for EnKF and PF. However, the results indicate that interactive effects occur among the three proportionality factors, suggesting that the effects of the three factors are dependent with each other. For instance, the interactive plot between forcing data and model predictions (the middle one in the first line in Figure (9c)) shows that the three lines of the forcing data increase as the proportionality factor in model predictions increases from 0.1 to 0.3. At the same time the solid line, representing the low level of proportionality factor in forcing data, increases faster than the other two lines when the proportionality factor of model predictions increases from 0.2 to 0.3, implying an interaction between this pair of factors. Figure 10 presents the fitted response surfaces with contour plots to reveal the interactions of

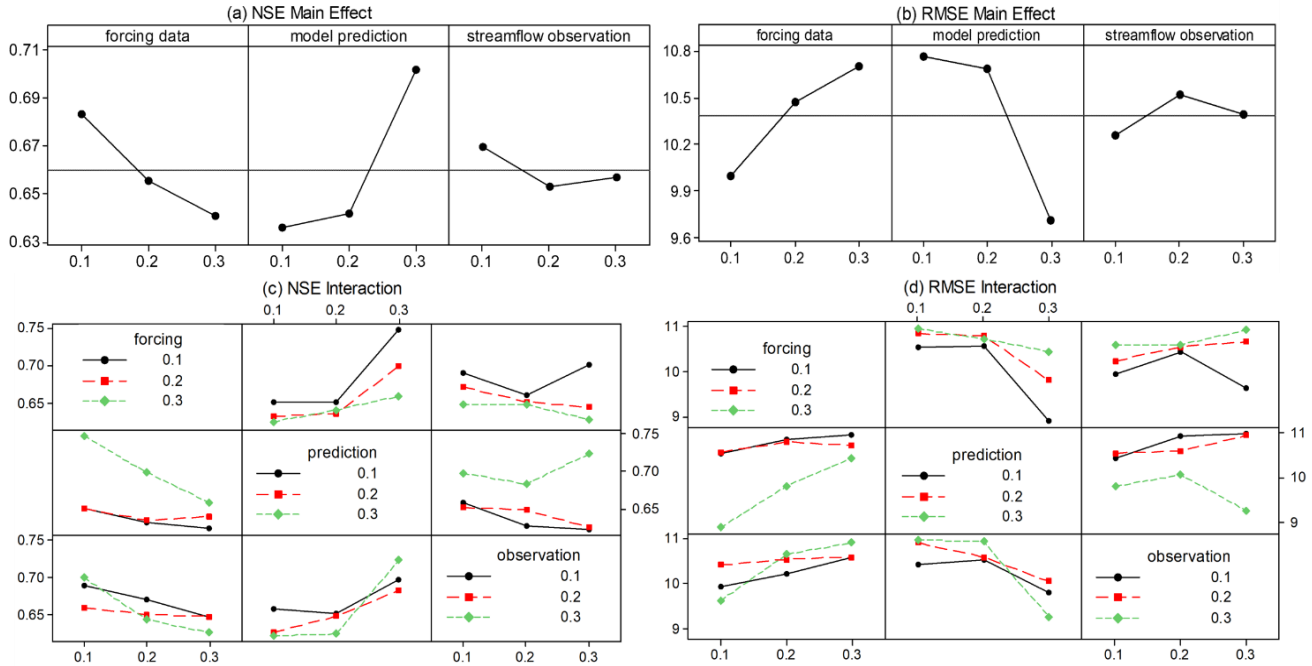


Figure 9. Main and interactive effects for the stochastic perturbations on the performance of CEnPF approach. Figures (14a) and (14b) indicate that the proportionality factor in model prediction poses the most significant impact on CEnPF with a higher proportionality factor value leading to a better performance. The intersection of the three lines in Figures (14c) and (14d) indicate that interactive effects occur for two factors at three levels. The broken lines imply the nonlinear relationship between stochastic perturbations and model performance.

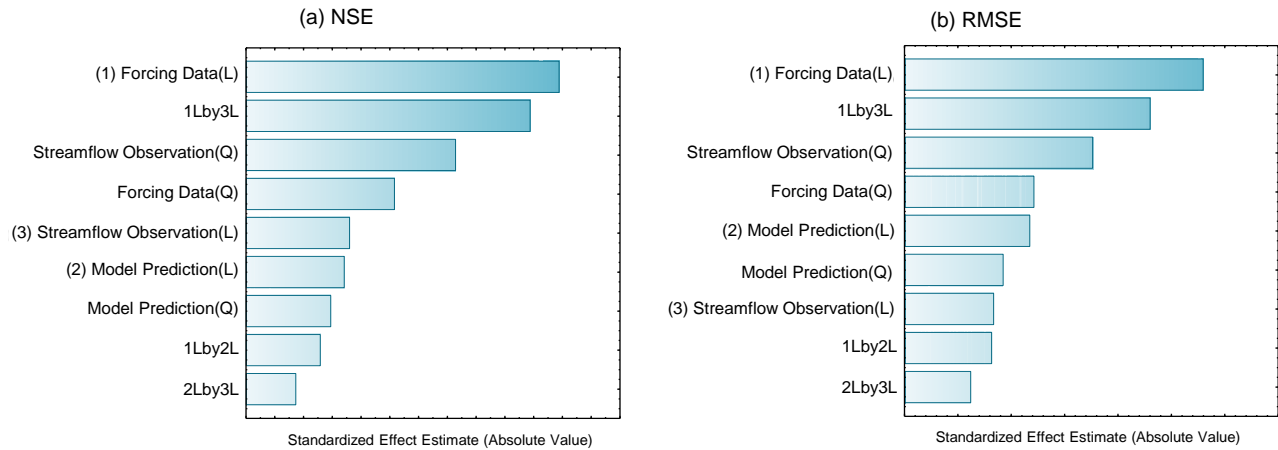


Figure 11. Pareto chart of standardized effects in terms of NSE (a) and RMSE (b) for PENPF. The random error in forcing data (i.e., factor (1)) influences the performance of PENPF most significantly, followed by the interaction of factor (1) and (3) (i.e., random error in streamflow observation), the quadratic effects of factors (1) and (3) (i.e., random error in streamflow observation), the linear effect of factors (3) and (2) (i.e., random error in model prediction), quadratic effect of interaction of factors (1) and (2), interaction of factor (1) and (3), linear main effect of factor (3), quadratic main effects of factors (3) and (1).

the three factors on the performance of CEnPF. These plots suggest that better performance of CEnPF can be achieved in the corner areas, implying that low random error in forcing data, and high random error in model predictions and streamflow observations may result in the best performances of CEnPF.

For the proposed CEnPF approach, the case study also demonstrates its better performance in hydrologic data assimilation

than traditional EnKF and PF methods. The impacts of random errors on CEnPF are different from those impacts of random errors on EnKF and PF. The random error in model predictions has a statistically significant impact on the performance of CEnPF. However, interactions among the three factors occur for CEnPF, and extreme random error scenarios may be more likely to lead to a better performance of CEnPF, which is simi-

lar for the processes of EnKF and PF.

4.4. Performance of PEnPF

For the case study application, the performance of PEnPF has a wider fluctuation under different combinations of stochastic perturbations in forcing data, model predictions and streamflow observations. As presented in Table 2, PEnPF can achieve

good performances with the NSE value larger than 0.8 in many scenarios, but it may also produce unsatisfactory results with an NSE value of 0.46. It may be concluded that PEnPF has many chances to produce better hydrologic predictions than traditional EnKF and PF. The ANOVA results for PEnPF are presented in Table 6. The results indicate that random errors in the forcing data have a statistically significant impact on the performance of PEnPF. Even though the impact from the random

Table 6. Results of ANOVA for PenPF

NSE	Degree of Freedom	SS	MS	F	P
forcing data	2	0.072791	0.036395	7.9	0.013
model prediction	2	0.003958	0.001979	0.43	0.665
streamflow observation	2	0.019033	0.009516	2.07	0.189
forcing data*model prediction	4	0.03543	0.008858	1.92	0.2
forcing data*streamflow observation	4	0.102592	0.025648	5.57	0.019
model prediction* streamflow observation	4	0.010684	0.002671	0.58	0.686
Error	8	0.036841	0.004605		
Total	26	0.28133			

RMSE	Degree of Freedom	SS	MS	F	P
forcing data	2	23.868	11.934	8.49	0.011
model prediction	2	1.761	0.88	0.63	0.559
streamflow observation	2	4.763	2.382	1.7	0.243
forcing data*model prediction	4	9.704	2.426	1.73	0.237
forcing data*streamflow observation	4	26.61	6.652	4.74	0.03
model prediction* streamflow observation	4	2.027	0.507	0.36	0.83
Error	8	11.239	1.405		
Total	26	79.972			

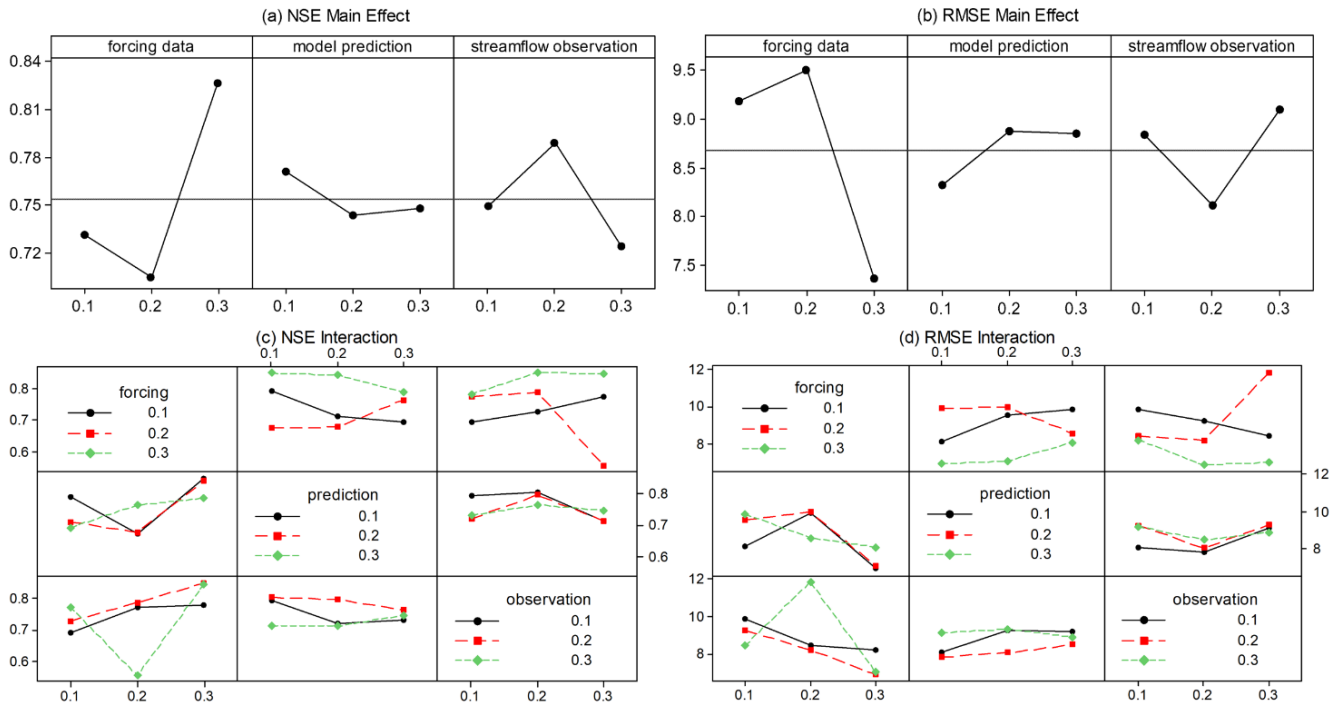


Figure 12. Main effects for the stochastic perturbations in forcing data, model prediction and streamflow observation on the performance of the PEnPF approach. For main effects, the random error in forcing data has the most significant impact (Figures (12a) and (12b)). The interaction plot matrix shows interactive effects occur among the three proportionality factors.

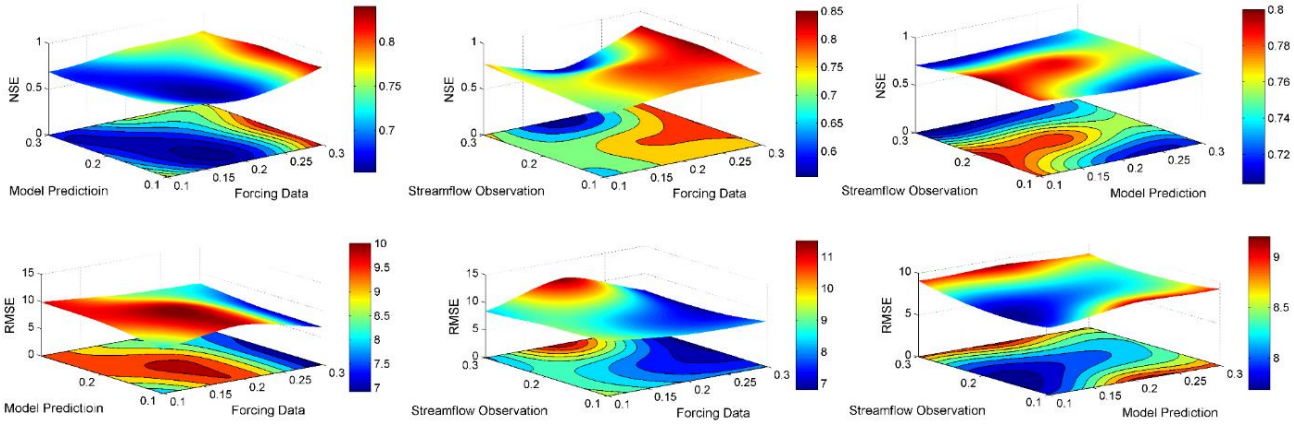


Figure 13. Fitted response surfaces with contour plots for the interactions among the three stochastic perturbation factors for PEnPF.

error in streamflow observation is insignificant, the interaction between random errors in forcing data and streamflow observation is statistically significant. Figure 11 shows the rank of the individual and joint effects of the three factors based on the Pareto chart. The linear main effect of the random error in forcing data is ranked as the most significant factor, followed by the interaction between random errors in forcing data and streamflow observation. This conclusion is consistent with the ANOVA results. Moreover, the Pareto charts for NSE and RMSE are similar with each other except for slight differences in the rank for some insignificant effects.

The main effect plots for the three factors and their interaction plot matrix are shown in Figure 12. The results exhibit great differences from the main effect and interaction plots for EnKF, PF, and CEnPF. It can be visualized that the randomness in forcing data has the greatest effect upon the performance of PEnPF, with a higher proportionality factor leading to a better performance. Also, the full interactions plot matrix (Figures 11b) and (11c) indicates that the three factors have interactive effects on PEnPF, which means that the magnitude of the effects of the three factors is dependent upon each other. Moreover, the fitted surfaces with the corresponding contour plots in Figure 13 indicate quadratic effects for the three factors. It is indicated that the proposed PEnPF may produce good predictions when the random errors in forcing data, model prediction, and streamflow observation are at their high level, low level and medium level, respectively.

For the developed PEnPF approach, the case study demonstrates that it may have many chances to achieve a better performance than EnKF and PF due to its capability of choosing better posterior estimates from EnKF and PF for each time step. The multi-level factorial results indicate that random error in forcing data has the greatest impact, which is also statistically significant. Interactions occur among the three factors, in which the interaction between random errors in forcing data and streamflow observation is statistically significant.

5. Conclusions

Sequential data assimilation (SDA) techniques have been

widely used uncertainty quantification and reduction in hydrologic prediction. In a data assimilation scheme, its performance is critically influenced by error estimates for the forcing data, output measurement, and model prediction. In this study, a multi-level factorial analysis approach has been employed to characterize the impacts of random error estimates on the performances of different data assimilation schemes. In detail, four data assimilation schemes were used, including EnKF and PF, as well as two integrated data assimilation approaches (i.e., CEnPF and PEnPF). Different levels of the proportional factor in the random error perturbation were assumed, and then the individual and interactive effects were visualized by the multi-level factorial analysis method.

The impacts of random errors on the performance of a data assimilation scheme were tested by a conceptual model in a catchment in the Jing River basin in China. Three random error scenarios were assumed for the forcing data, streamflow observations and model predictions, leading to a multi-level factorial analysis (i.e., 3^3 factorial analysis) framework. The results indicated that different stochastic perturbations in model inputs, outputs and streamflow observations had different contributions on the selected data assimilation schemes, and some stochastic perturbations and their interactions may be statistically insignificant. But a data assimilation scheme may be more likely to achieve good performance when the proportionality factors in random errors are at their extreme levels (i.e., low or high levels).

As an extension of the first paper, this study used a multi-level factorial analysis approach to characterize the impacts of random perturbations on the data assimilation process and to reveal the main and interactions of stochastic perturbations on different data assimilation schemes. Through this research, it can be found that (i) the new developed CEnPF and PEnPF approaches in the first paper can provide more accurate predictions than EnKF and PF in most scenario combinations of random errors; (ii) for all selected data assimilation schemes, they are more likely to achieve good performances when the random errors are at their low or high levels.

Acknowledgement. This research was supported by the National Key Research and Development Plan (2016YFA0601502), and the Royal

Society International Exchanges Program (No. IES\R2\202075)

References

- Clark, M.P., Rupp, D.E., Woods, R.A., Zheng, X., Ibbitt, R.P., Slater, A.G., Schmidt, J., and Uddstrom, M.J. (2008). Hydrological data assimilation with the ensemble Kalman filter: Use of streamflow observations to update states in a distributed hydrological model. *Adv. Water Resour.*, 31(10), 1309-1324. <https://doi.org/10.1016/j.advwatres.2008.06.005>
- Clark, M.P. and Slater, A.G. (2006). Probabilistic quantitative precipitation estimation in complex terrain, *J. Hydrometeorol.* 7(1), 3-22. <https://doi.org/10.1175/JHM474.1>
- Dong, C., Huang, G.H., and Cheng, G.H. (2021). Offshore wind can power Canada. *Energy*, 121422. <https://doi.org/10.1016/j.energy.2021.121422>
- Crow, W.T. and Van Loon, E. (2006). Impact of incorrect model error assumptions on the sequential assimilation of remotely sensed surface soil moisture. *J. Hydrometeorol.*, 7(3), 421-432. <https://doi.org/10.1175/JHM499.1>
- Fan, Y.R., Huang, G.H., Baetz, B.W., Li, Y.P., Huang, K., Li, Z., Chen, X., and Xiong, L.H. (2016). Parameter uncertainty and temporal dynamics of sensitivity for hydrologic models: A hybrid sequential data assimilation and probabilistic collocation method. *Environ. Model. Softw.*, 86(3), 30-49. <https://doi.org/10.1016/j.envsoft.2016.09.012>
- Fan, Y.R., Huang, G.H., Baetz, B.W., Li, Y.P., Huang, K., Chen, X., and Gao, M. (2017a). Development of integrated approaches for hydrological data assimilation through combination of ensemble kalman filter and particle filter methods. *J. Hydrol.*, 550, 412-426. <https://doi.org/10.1016/j.jhydrol.2017.05.010>
- Fan, Y.R., Huang, G.H., Baetz, B.W., Li, Y.P., and Huang, K. (2017b). Development of a copula-based particle filter (CopPF) approach for hydrologic data assimilation under consideration of parameter interdependence. *Water Resour. Res.*, 53 (6), 4850-4875. <https://doi.org/10.1002/2016WR020144>
- Fan, Y.R., Huang, G.H., Baetz, B.W., Li, Y.P., and Huang, K. (2020a). Uncertainty characterization and partition in multivariate risk inference: a factorial bayesian copula framework. *Environ. Res.*, 183(1), 109215. <https://doi.org/10.1016/j.envres.2020.109215>
- Fan, Y.R., Huang, G.H., Huang, K., and Wang, F. (2020b). An uncertainty partition approach for inferring interactive hydrologic risks. *Hydrol. Earth Syst. Sci.*, 24(9), 4601-4624. <https://doi.org/10.5194/hess-24-4601-2020>
- Fan, Y.R., Huang, W.W., Li, Y.P., Huang, G.H., and Huang, K. (2015a). A coupled ensemble filtering and probabilistic collocation approach for uncertainty quantification of hydrological models. *Journal of Hydrology*, 530, 255-272. <https://doi.org/10.1016/j.jhydrol.2015.09.035>
- Fan, Y.R., Huang, W.W., Huang, G.H., Huang, K., and Zhou, X. (2015b). A PCM-based stochastic hydrological model for uncertainty quantification in watershed systems. *Stoch Environ. Res. Risk Assess.*, 29(3), 915-927. <https://doi.org/10.1007/s00477-014-0954-8>
- Fan, Y.R., Yu, L., and Shi, X. (2021). Uncertainty Quantification and partition for multivariate risk inferences through a factorial multi-model Bayesian copula (FMBC) System. *J. Hydrol.*, 598(3), 1264-06. <https://doi.org/10.1016/j.jhydrol.2021.126406>
- Fu, Y.P., Huang, G.H., Liu, L.R. and Zhai, M.Y. (2021). A factorial CGE model for analyzing the impacts of stepped carbon tax on Chinese economy and carbon emission. *Sci. Total Environ.*, 759, 143512. <https://doi.org/10.1016/j.scitotenv.2020.143512>
- Georgakakos, K.P., Seo, D.J., Gupta, H., Schaake, J., and Butts, M.B. (2004). Towards the characterization of streamflow simulation uncertainty through multimodel ensembles. *J. Hydrol.*, 298(1-4), 222-241. <https://doi.org/10.1016/j.jhydrol.2004.03.037>
- Gätzing, J. and Bárdossy, A. (2009). Generic error model for calibration and uncertainty estimation of hydrological models. *Water Resour. Res.*, 44(12), 1393-1442. <https://doi.org/10.1029/2007WR006691>, 2008
- Hong, Y., Hsu, K.L., Moradkhani, H., and Sorooshian, S. (2006). Uncertainty quantification of satellite precipitation estimation and Monte Carlo assessment of the error propagation into hydrologic response. *Water Resour. Res.*, 42(8), W08421. <https://doi.org/10.1029/2005WR004398>
- Komma, J., Bloschl, G., and Reszler, C. (2008). Soil moisture updating by Ensemble Kalman Filtering in real-time flood forecasting. *J. Hydrol.*, 357(3-4), 228-242. <https://doi.org/10.1016/j.jhydrol.2008.05.020>
- Leisenring, M. and Moradkhani, H. (2012). Analyzing the uncertainty of suspended sediment load prediction using sequential data assimilation. *J. Hydrol.*, 468, 268-28. <https://doi.org/10.1016/j.jhydrol.2012.08.049>
- Li, Y.F., Li, Y.P., Huang, G.H. and Chen, X. (2010). Energy and environmental systems planning under uncertainty—an inexact fuzzy-stochastic programming approach. *Appl. Energy*, 87(10), 3189-3211. <https://doi.org/10.1016/j.apenergy.2010.02.030>
- Li, Y.P., Huang, G.H., Yang, Z.F. and Nie, S.L. (2008). IFMP: Interval-fuzzy multistage programming for water resources management under uncertainty. *Resour. Conserv. Recy.*, 52(5), 800-812. <https://doi.org/10.1016/j.resconrec.2007.11.007>
- Liu, Y., Weerts, A.H., Clark, M., Hendricks Franssen, H.J., Kumar, S., Moradkhani, H., Seo, D.J., Schwanenber, D., Smith, P., van, Dijk A.I.J.M., van Velzen, N., He, M., Lee, H., Noh, S.J., Rakovec, O., and Restrepo, P. (2012). Advancing data assimilation in operational hydrologic forecasting: progresses, challenges, and emerging opportunities. *Hydrol. Earth Syst. Sci.*, 16(10), 3863-3887. <https://doi.org/10.5194/hess-16-3863-2012>
- Montgomery, D.C. (2000). *Design and analysis of experiments (5th ed.)*. John Wiley and Sons. ISBN: 978-1-118-14692-7
- Moor, R.J. (2007). The PDM rainfall-runoff model. *Hydrol. Earth Syst. Sci.*, 11 (1), 483-499. <https://doi.org/10.5194/hess-11-483-2007>
- Moradkhani, H., Sorooshian, S., Gupta, H.V., and Houser, P. (2005a). Dual state – parameter estimation of hydrologic models using ensemble Kalman filter. *Adv. Water Resour.*, 28(2), 135-147. <https://doi.org/10.1016/j.advwatres.2004.09.002>
- Moradkhani, H., Hsu, K.L., Gupta, H., and Sorooshian, S. (2005b). Uncertainty assessment of hydrologic model states and parameters: Sequential data assimilation using the particle filter. *Water Resour. Res.*, 41(5), W05012. <https://doi.org/10.1029/2004WR003604>
- Pan, M. and Wood, E.F. (2009). A multiscale ensemble filtering system for hydrologic data assimilation. Part II: Application to land surface modeling with satellite rainfall forcing. *J. Hydrometeorol.*, 10(6), 1493-1506. <https://doi.org/10.1175/2009JHM1155.1>
- Parrish, M., Moradkhani, H., and DeChant, C.M. (2012). Towards reduction of model uncertainty: integration of bayesian model averaging and data assimilation. *Water Resour. Res.*, 48(3), W03519. <https://doi.org/10.1029/2011WR011116>
- Pathiraja, S., Marshall, L., Sharma, A., and Moradkhani, H. (2016a). Detecting non-stationary hydrologic model parameters in a paired catchment system using data assimilation. *Adv. Water Resour.*, 94(8), 103-119. <https://doi.org/10.1016/j.advwatres.2016.04.021>
- Pathiraja, S., Marshall, L., Sharma, A., and Moradkhani, H. (2016b). Hydrologic modeling in dynamic catchments: a data assimilation approach. *Water Resour. Res.*, 52(5), 3350-3372. <https://doi.org/10.1002/2015WR017192>
- Pauwels, V.R. and De Lannoy, G.J. (2006). Improvement of modeled soil wetness conditions and turbulent fluxes through the assimilation of observed discharge. *J. Hydrometeorol.*, 7(3), 458-477. <https://doi.org/10.1175/JHM490.1>
- Reichle, R., Mclaughlin D., and Entekhabi D. (2002). Hydrologic data assimilation with the ensemble Kalman filter. *Mon. Weather Rev.*, 130(1), 103-114. [https://doi.org/10.1175/1520-0493\(2002\)130<0103:0130.0](https://doi.org/10.1175/1520-0493(2002)130<0103:0130.0)

CO;2

- Steiner, M. (1996). Uncertainty of estimates of monthly areal rainfall for temporally sparse remote observations. *Water Resour. Res.*, 32(2), 373-388. <https://doi.org/10.1029/95WR03396>
- Tan, Q., Huang, G.H. and Cai, Y.P. (2011). Radial interval chance-constrained programming for agricultural non-point source water pollution control under uncertainty. *Agric. Water Manag.*, 98(10), 1595-1606. <https://doi.org/10.1016/j.agwat.2011.05.013>
- Vrugt, J.A., Gupta, H.V., Bouten, W., and Sorooshian, S. (2003). A shuffled complex evolution metropolis algorithm for optimization and uncertainty assessment of hydrologic model parameters. *Water Resour. Res.*, 39(8), 1201. <https://doi.org/10.1029/2002WR001642>
- Vrugt, J.A., Diks, C.G.H., Gupta, H.V., Bouten, W., and Verstraten, J.M. (2005). Improved treatment of uncertainty in hydrologic modelling: combining the strengths of global optimization and data assimilation. *Water Resour. Res.*, 41(1), W01017. <https://doi.org/10.1029/2004WR003059>
- Wang, S., Huang, G.H., Huang, W., Fan, Y.R., and Li, Z. (2015). A fractional factorial probabilistic collocation method for uncertainty propagation of hydrologic model parameters in a reduced dimensional space. *J. Hydrol.*, 529(3), 1129-1146. <https://doi.org/10.1016/j.jhydrol.2015.09.034>
- Weerts, A.H. and Serafy, G.Y.H.E. (2006). Particle filtering and ensemble Kalman filtering for state updating with hydrological conceptual rainfall-runoff models. *Water Resour. Res.*, 42(9), 123-154. <https://doi.org/10.1029/2005WR004093>
- Xie, X. and Zhang, D. (2013). A partitioned update scheme for state-parameter estimation of distributed hydrologic models based on the ensemble Kalman filter. *Water Resour. Res.*, 49(11), 7530-7365. <https://doi.org/10.1002/2012WR012853>